

# Radio spectroscopy of the optically aligned spin states of color centers in silicon carbide

V A Soltamov, P G Baranov

DOI: 10.3367/UFNe.2016.02.037755

## Contents

1. Introduction	605
2. Spin color centers in silicon carbide as a promising basis for the spectroscopy of quantum systems with controllable quantum states	606
3. Conclusions	610
References	610

**Abstract.** The unique quantum properties of nitrogen-vacancy color centers (NV centers) in diamond have motivated the search for similar color centers with enhanced properties in SiC. In this paper, experimental evidence is presented that vacancy-related spin centers in SiC not only have properties similar to those of diamond NV centers but also exhibit many additional properties, making these quantum systems promising for various applications in spintronics, sensorics, and quantum information processing under ambient conditions.

**Keywords:** spin centers, silicon vacancy-related centers, optical polarization of electron spins, magnetic resonance

## 1. Introduction

Electron paramagnetic resonance (EPR), which was discovered by Zavoisky [1] in Kazan in 1944, is one of the most powerful analytical tools available to physicists, chemists, and biologists. EPR-based radiospectroscopy methods like electron spin echo (ESE), optical detection of magnetic resonance (ODMR), and detection of electron–nuclear double resonance (ENDOR) are the most informative instruments for investigating the structural and spin properties of condensed systems, living matter, and nanostructures and nanobiotechnology objects. One of the main lines of modern technology developments is the miniaturization of micro- and optoelectronic components. Any device with nanodimensional characteristics is bound to exhibit elements of quantum behavior. Spin is a purely quantum-mechanical object, and therefore spin effects begin to play a decisive role in the development of different instruments and devices

involving nanodimensional structures. In this case, magnetic resonance techniques provide a basis for the study of spin effects in nature, of nondestructive monitoring, and of diagnostics of materials. Due to their relatively low sensitivity, traditional EPR and nuclear magnetic resonance (NMR) methods have a limited application for investigating systems with a small number of spin moments. The main requirement in the study of such systems is improvement of the magnetic resonance sensitivity, which is possible only by increasing the working frequencies or employing optical (electrical) methods of magnetic resonance detection. This is the reason why EPR- and NMR-spectroscopy techniques have developed rapidly in recent years toward higher microwave frequencies and the use of double resonances.

The growing interest in manipulating the spin states of electrons and nuclei in semiconductors and semiconductor nanostructures is due to possible applications in spintronics for quantum information processing in the new generation of supersensitive quantum magnetometers, quantum thermometers, and biosensors with submicrometer spatial resolution. The last decade has seen an explosive growth in experimental and theoretical research in the area of quantum computing. The advantage of quantum computing over the classical one lies in the exponential speeding-up of a number of calculations, for instance, Fourier transformations and searches in unordered databases. The dimensions of modern computer chips are approaching the atomic scale, which generates the necessity of taking the quantum properties of the relevant atomic-sized structures into account.

Until recently, the practical applications of semiconductors involved the use of charge- and spin-carrier ensembles. The capability to efficiently control spin states is the key question of semiconductor spintronics. The unique quantum properties of nitrogen-vacancy (NV) color centers in diamond [2] have opened a new era in spintronics: it has become possible to manipulate the spin states of a single atomic-sized center at room temperature using optically detected magnetic resonance. An NV center is a nearest-neighbor pair of a nitrogen atom, which replaces a carbon atom, and a lattice vacancy. A unique optically induced spin-dependent cycle is

V A Soltamov, P G Baranov Ioffe Institute, Russian Academy of Sciences, ul. Politekhnikeskaya 26, 194021 Saint Petersburg, Russian Federation  
E-mail: pavel.baranov@mail.ioffe.ru

Received 7 March 2016  
Uspekhi Fizicheskikh Nauk 186 (6) 678–684 (2016)  
DOI: 10.3367/UFNr.2016.02.037755  
Translated by E N Ragozin; edited by A M Semikhatov

possible here in which the spin level populations are aligned in the ground triplet ( $S = 1$ ) spin state under unpolarized light in ambient conditions (at room temperature or even at temperatures exceeding room temperature by several hundred degrees). Any change in spin level populations (under an external resonance microwave field or internal processes due to cross relaxation or an anticrossing of spin levels) in turn leads to changes in the optical cycle, for instance, in the photoluminescence intensity. Owing to the huge difference in microwave and optical photon energies, a change in the optical photon intensity in the absorption of a microwave photon results in a giant improvement in the sensitivity of spin state detection, which makes it possible to record extremely small ensembles of the centers, down to single spins. Until recently, an NV center was the only known solid-state system in which such spin manipulations were possible [3–8].

However, there are several problems in using the centers in diamond. The main one is the technological problem of fabricating diamond-based devices, the boundedness of the optical range of NV center fluorescence in diamond, which is poorly compatible with fiber optics and the transmittance band of biological objects, and the difficulties of electrical spin control. The search for structures that exhibit unique quantum properties similar to those of NV centers in diamond and at the same time have much broader functional capabilities is a highly promising task.

## 2. Spin color centers in silicon carbide as a promising basis for the spectroscopy of quantum systems with controllable quantum states

The most promising material that may compete with diamond from the standpoint of spectroscopy of quantum systems is silicon carbide (SiC). Silicon carbide is a wide-gap semiconductor; its fabrication technology is well developed and permits producing perfect large-diameter plates with atomic-scale surface nonuniformities. These plates have the chemical, electrical, and mechanical properties that permit using this material in extreme conditions.

In nature, silicon carbide, which is known as carborundum, was first discovered in a meteorite late in the 19th century. A special feature of silicon carbide is the existence of its different polytypes. Most called-for among them are the cubic polytype 3C, the hexagonal polytypes 4H and 6H, and the rhombic polytype 15R. To distinguish the polytypes, we hereinafter use Ramsdell's notation, which indicates the number of layers in an elementary crystal cell and the type of its symmetry. There are more than 250 structural modifications of SiC; although all silicon carbide polytypes consist of 50% silicon and 50% carbon atoms, each polytype has features of its own. Therefore, for each of the polytypes, the properties of spin color centers are unique; furthermore, even in one polytype, the center may be located in different nonequivalent positions in the lattice.

Figure 1 shows the crystal lattice structure of two silicon carbide polytypes: hexagonal 6H-SiC and rhombic 15R-SiC; the plane of the drawing coincides with the (11–20) crystal plane. Symbols h and k denote the hexagonal and quasi-cubic positions of Si (C) atoms in the lattice. For instance, in 6H-SiC, there are three nonequivalent positions: one hexagonal (h) and two quasi-cubic (k1, k2). Shown for 6H-SiC are the possible models of the family of spin color centers in the form

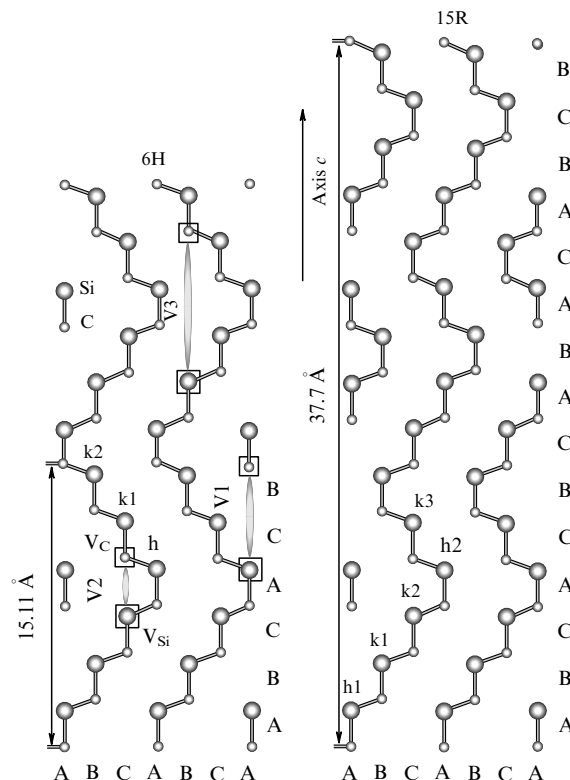


**Figure 1.** Crystal lattice structure of two polytypes of silicon carbide: hexagonal 6H-SiC and rhombic 15R-SiC. Symbols A, B, and C correspond to different positions of Si and C atoms in the close-packed hexagonal structure. The lengths of elementary cells are indicated: 15.11 and 37.7 Å.

of a negatively charged silicon vacancy ( $V_{Si}^-$ ) located along the  $c$ -axis and having no molecular bonds with the neutral carbon vacancy ( $V_C^0$ ). The V1, V2, and V3 center notation corresponds to the identification of zero-phonon luminescence lines adopted earlier. Similar models may be realized in the polytype 15R-SiC (not shown in the drawing), with a large number of possible structures anticipated due to the rhombic symmetry. By varying the position of the center in the crystal lattice, it is possible to change its properties. This allows choosing the center with parameters (for instance, optical and microwave ranges) suited to a specific problem.

Already 35 years ago, the discovery was made of the optically induced alignment (polarization) of spin levels of different color centers in a 6H-SiC crystal at a temperature of 77 K; the centers were produced by quenching crystals from a high temperature [9, 10]. More recently, these color centers were investigated in Refs [11–19], which showed that as in the case of NV centers, optically induced spin alignment takes place in the ground high-spin state. In this case, one family of color centers in the form of neighboring silicon–carbon divacancies with a molecular bond has a triplet ground state ( $S = 1$ ). Another family, that of negatively charged silicon vacancies perturbed by neutral carbon vacancies located along the  $c$ -axis at different distances from the silicon vacancy and having no molecular bonds to it (see Fig. 1), has a quadruplet spin ground state ( $S = 3/2$ ).

The authors of Refs [16, 18, 19] proposed the idea of considering spin color centers as candidates for the room-temperature spectroscopy of individual spins with controllable quantum states.

Beginning in 2010, after the publication of Refs [20, 21], which proposed searching for NV centers in silicon carbide,<sup>1</sup> the search for color centers in silicon carbide as an alternative to NV centers in diamond was started; in the last five years, the studies of spin color centers in silicon carbide broadened in an explosive manner (see, e.g., Refs [22–31]).

Several experimental techniques are used to investigate the optical and spin properties of color centers:

(1) photoluminescence (PL), in which confocal optics is typically used to mark out small crystal volumes with a focused laser beam. It is in this volume that the spin color centers are excited and the spin levels are aligned. Photoluminescence from this volume is recorded and the magnetic resonance is optically detected from PL intensity variations. For low color center densities, it is possible to extract the luminescence of individual spin centers;

(2) EPR, which is an important technique for investigating the local environment of paramagnetic centers and their spin properties. The experimental results described in this paper were obtained with spectrometers in different frequency ranges: X (9.5 GHz), Q (35 GHz), and W (95 GHz), both in the continuous mode and in the electron spin echo mode;

(3) ENDOR, in which transitions between nuclear levels (NMR) are recorded from variations of the ESE signal;

(4) direct-detected EPR (DD-EPR), which is used for extracting optically sensitive signals; in this case, the signals excited by an optical pulse are measured in the absorption or emission mode;

(5) optically detected magnetic resonance, which is determined from PL intensity variations.

For example, Fig. 2 shows zero-phonon lines (ZPLs) in photoluminescence spectra V1, V2, V3, and V4 observed at low temperatures, which correspond to different spin color centers in 6H-SiC and 15R-SiC polytypes. Observed in the 6H-SiC and 15R-SiC polytypes are three and four ZPLs, respectively (two ZPLs, V1 and V2, were observed in the 4H-SiC polytype). The values of ZPL energies are collected in Table 1.

As an example, we consider the family of uniaxially aligned spin color centers with the quadruplet spin ground state ( $S = 3/2$ ), which was recently discovered in the rhombic 15R-SiC polytype of silicon carbide [31].

To uniquely attribute the EPR signals of spin centers to the ZPLs shown in Fig. 2, experiments were done to directly detect the EPR signals induced by an optical flash with the energy corresponding to a ZPL.

Figure 3a shows the EPR signals induced by an optical flash with energies corresponding to the ZPLs V2, V3, and V4

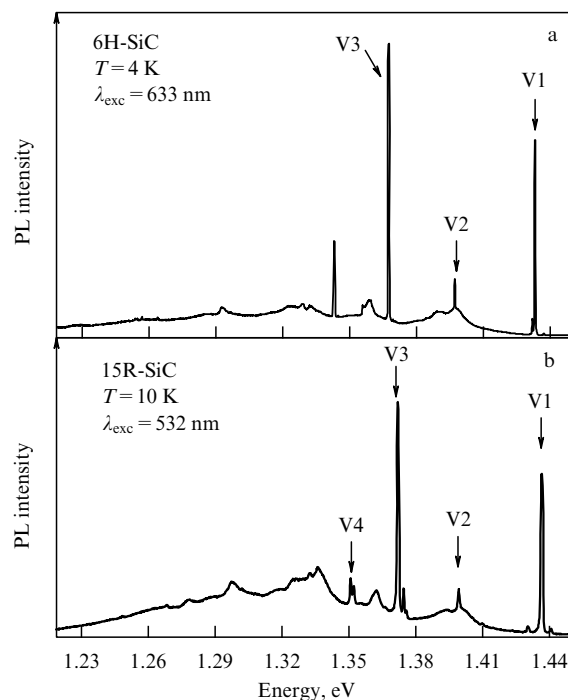


**Figure 2.** Photoluminescence spectra recorded at the temperature  $T = 10$  K in (a) 6H-SiC and (b) 15R-SiC. The ZPLs of silicon vacancy centers are denoted as V1–V4.

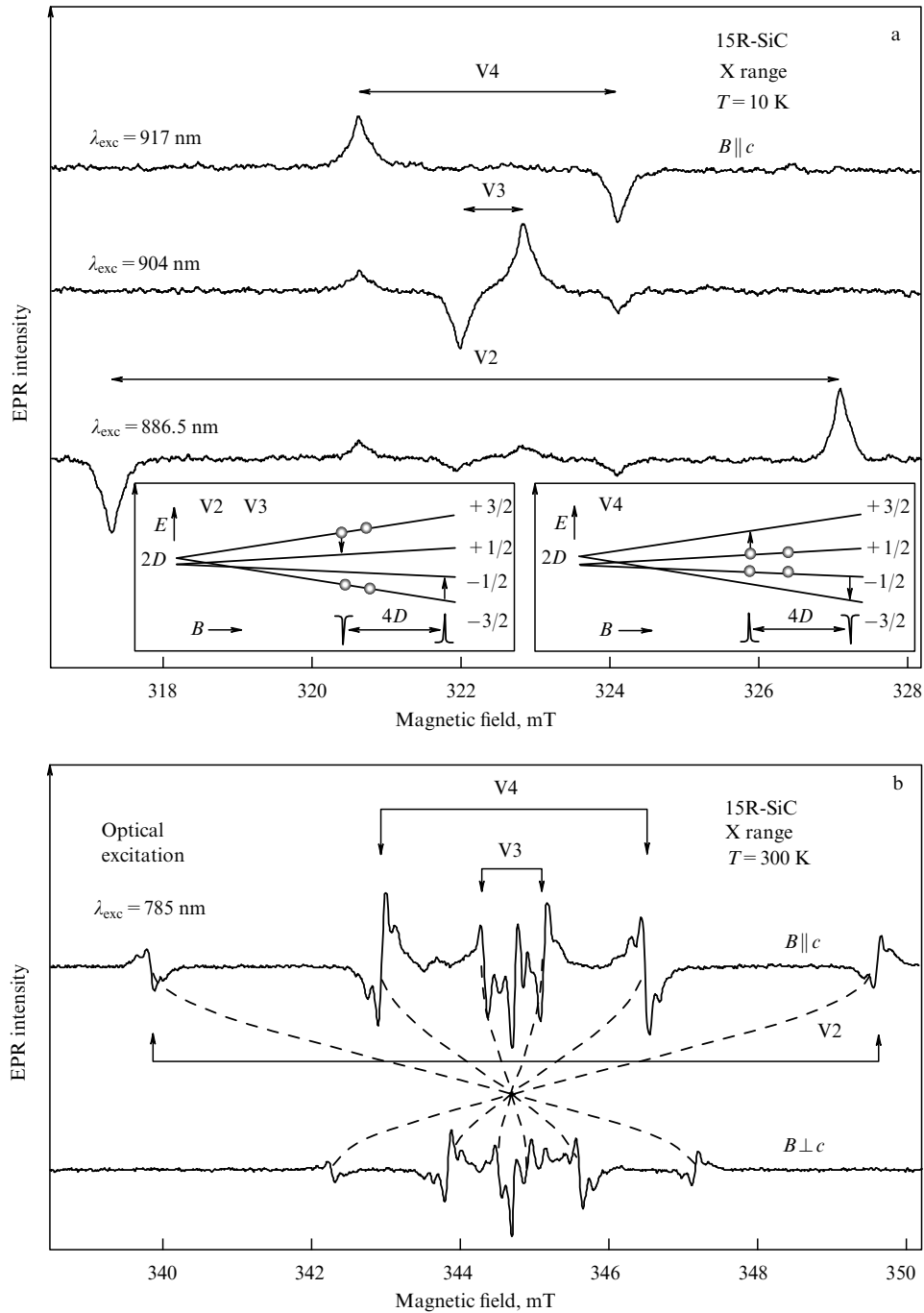
(see Fig. 2) in 15R-SiC. Different phases of the low- and high-field EPR signals caused by the optical alignment of different pairs of spin levels in the  $S = 3/2$  system can be seen. Time-resolved EPR signals induced by an optical flash uniquely relate the optical lines of spin color centers to EPR spectra. The insets in Fig. 3a show energy level diagrams for the magnetic field orientation along the crystal  $c$ -axis for centers with two types of optical alignment of spin levels: in the case of V2 and V3 centers, the upper levels are primarily populated (in the zero magnetic field, these populations are also retained in a nonzero magnetic field); in the case of V4 centers, the lower levels are primarily populated.

Figure 3b shows the EPR spectra recorded in the X range at room temperature under continuous optical excitation by an infrared (IR) laser at a wavelength of 785 nm, which are presented for two orientations,  $B \parallel c$  and  $B \perp c$ . The curves show the orientational dependences in the rotation of the magnetic field vector between these orientations. The symmetrically located satellites of each line are caused by hyperfine interactions with 12 silicon atoms of the second coordination sphere around the negatively charged silicon vacancy. The dark EPR spectra in the absence of optical excitation are less intense by about two orders of magnitude and have the same phases.

<sup>1</sup> We note that DiVincenzo's paper [21] bears an inspirational title: "Quantum bits: Better than excellent."

**Table 1.** Optical transition energies (wavelengths) for ZPLs at a temperature of 4 K; fine structure splitting parameters  $\Delta$  in the zero magnetic field and  $g$  factors of the family of V1, V2, V3, and V4 spin color centers for nonequivalent positions in the crystal lattices of the 4H-SiC, 6H-SiC, and 15R-SiC polytypes.

Polytype	4H-SiC		6H-SiC			15R-SiC		
Zero-phonon line	V1	V2	V1	V2	V3	V2	V3	V4
$E$ , eV/ $\lambda$ , nm	1.438/862	1.352/917	1.433/865	1.397/887	1.368/906	1.399/886.5	1.372/904	1.352/917
$\Delta$ , MHz/v, $\text{cm}^{-1}$	39/13	66/22	27/9	128/42.7	27/9	139.2/46.4	11.6/3.87	50.2/16.7



**Figure 3.** (a) EPR signals induced by an optical flash with energies corresponding to the ZPLs V2, V3, and V4 (see Fig. 2) in 15R-SiC. (b) EPR spectra recorded at room temperature in the X band under continuous optical excitation at a wavelength of 785 nm by an IR laser.

EPR spectra are described by the standard spin Hamiltonian with an axial symmetry with the spin  $S = 3/2$ :

$$H = g_e \mu_B \mathbf{B} \mathbf{S} + D \left[ S_z^2 - \frac{1}{3} S(S+1) \right].$$

Here,  $g_e \approx 2.0$  is the electron  $g$  factor (see Table 1),  $\mu_B$  is the Bohr magneton,  $S_z$  is the operator of the total spin  $S$  projection on the symmetry axis of the center (in the case of the centers under consideration here, this is the  $c$ -axis of the SiC crystal; the symmetry of the centers is  $C3v$ ), and  $D$  is the parameter for describing the fine structure in the axial crystal field. In the zero magnetic field ( $B = 0$ ), the ground state for

$S = 3/2$  is split into two degenerate sublevels:  $M_S = \pm 1/2$  and  $M_S = \pm 3/2$ . The separation of these spin sublevels is equal to the fine structure splitting  $\Delta$  in a zero magnetic field; for the spin  $S = 3/2$ ,  $\Delta = 2D$ . The splitting  $\Delta$  is different for different centers and depends on the polytype and the spin-center position in the crystal lattice (see Table 1). A similar splitting is also observed in the excited state.

Using the high-frequency spin-echo and electron–nuclear double resonance techniques, it was possible to determine the structure of the family of these spin color centers at the electron level and, from the analysis of hyperfine interactions with silicon and carbon atoms, to obtain information about the spatial distribution of the

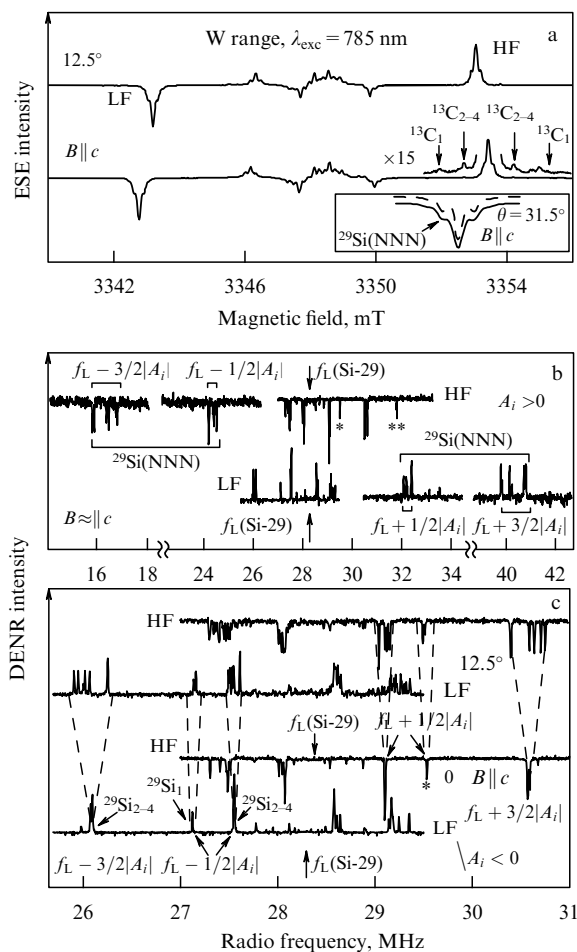
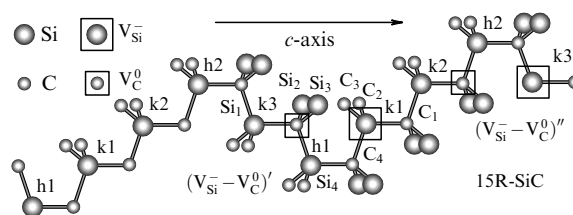


**Figure 4.** (a) Spectra of electron spin echo (ESE) measured in the W range. (b, c) ENDOR spectra recorded from the ESE for low-field (LF) and high-field (HF) transitions indicated by arrows in Fig. 4a.

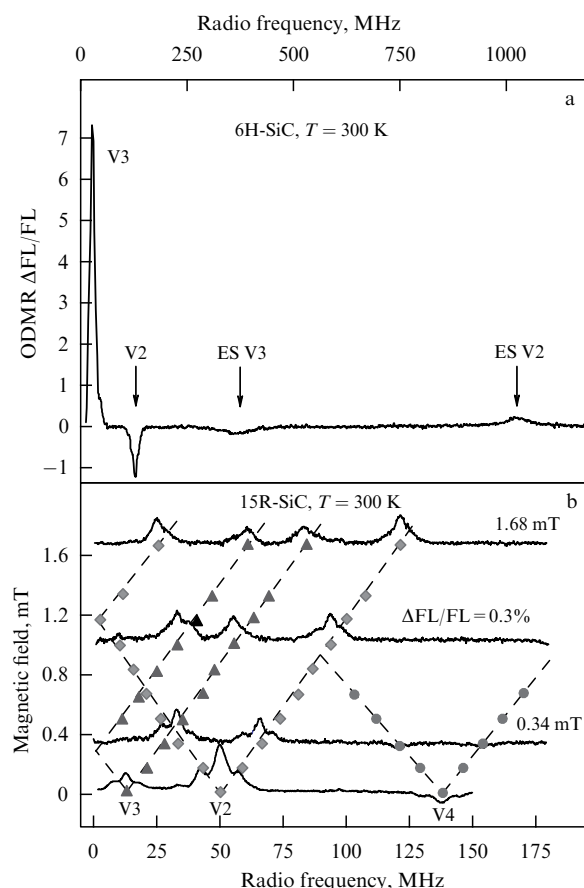
electron spin density on the nearest coordination spheres in the crystal lattice.

Figure 4a shows the ESE spectra measured in the W range (95 GHz) in a 15R-SiC crystal for two angles,  $\theta = 0$  ( $B \parallel c$ ) and  $\theta = 12.5^\circ$ , between the vector of the external magnetic field and the  $c$ -axis of the crystal under continuous optical excitation by an IR laser at a wavelength of 785 nm. The inset in Fig. 4a is a zoom-in of the low-field EPR transition in two orientations for demonstrating the orientational dependence of the linewidths of fine structure components. This is attributable to the existence of anisotropic ENDOR lines corresponding to the interaction with silicon atoms in the first coordination sphere of the neutral carbon vacancy, which is a part of the spin center.

To determine the structure of spin centers, an investigation was made of the ENDOR spectra recorded from a variation of ESE signals on application of a signal with the radio frequency corresponding to transitions between NMR levels. Figures 4b and 4c show the ENDOR spectra recorded from the ESE for the low-field (LF) and high-field (HF) transitions indicated by arrows in Fig. 4a. The transitions corresponding to the frequencies  $f_L + 1/2|A_i|$  and  $f_L + 3/2|A_i|$  for hyperfine interactions with the axial silicon atoms in the first coordination sphere of the neutral carbon vacancy  $V_C^0$  are respectively marked with one and two asterisks.  $^{29}\text{Si}_1$  and  $^{29}\text{Si}_{2-4}$  denote the ENDOR lines



**Figure 5.** Detail of the 15R-SiC crystal structure.



**Figure 6.** (a) ODMR signals of V2 and V3 spin color centers ( $S = 3/2$ ) recorded in a 6H-SiC crystal in a zero magnetic field. (b) ODMR signals of V2, V3, and V4 centers in a 15R-SiC crystal for different values of the external magnetic field.

corresponding to the presence of  $^{29}\text{Si}$  atoms in the first coordination sphere of the neutral carbon vacancy  $V_C^0$ . Based on these investigations, a model was proposed for the structure of the family of centers with the spin  $S = 3/2$  in the ground and excited states (Fig. 5).

Figure 5 shows a detail of the 15R-SiC crystal structure with two hexagonal ( $h1, h2$ ) and three quasi-cubic ( $k1, k2, k3$ ) positions of silicon (carbon). The vacancies are indicated by squares. The structure of the center is a negatively charged silicon vacancy ( $V_{\text{Si}}^-$ ) and a neutral carbon vacancy ( $V_C^0$ ), which is positioned on the  $c$ -axis and has no molecular bond; the spin of the center is  $S = 3/2$  in the ground and excited states. The carbon atoms in the first coordination sphere of the negatively charged silicon vacancy are denoted by  $C_{1-4}$ , the silicon atoms in the first coordination sphere of the neutral carbon vacancy by  $Si_{1-4}$ , and the V2-center structures of two types by  $(V_{\text{Si}}^- - V_C^0)'$  and  $(V_{\text{Si}}^- - V_C^0)''$ .

Figure 6a shows the ODMR signals of the spin color centers V2 and V3 ( $S = 3/2$ ) recorded at room temperature in a 6H-SiC crystal under 785 nm laser excitation in a zero magnetic field. The signals denoted by ES V3 and ES V2 correspond to the excited states of the V3 and V2 centers with the spin  $S = 3/2$ .

Figure 6b shows the ODMR signals of the centers V2, V3, and V4 recorded at room temperature in a 15R-SiC crystal under 785 nm laser excitation for different values of the external magnetic field (the lower spectrum was recorded in an external magnetic field of about 0.5 G to cancel Earth's magnetic field). The vertical mark indicates the ODMR contrast magnitude, i.e., the relative intensity change of spin-center luminescence under conditions of magnetic resonance. Given for each center are the dependences of the signal position on the magnetic field — an effect employed in a quantum magnetometer.

It was shown that these centers have unique characteristics like the optically induced alignment of spins at temperatures up to 250 °C with a record contrast factor, which is extremely important for applications.

### 3. Conclusions

The last five years have seen the demonstration of unique characteristics of spin color centers in silicon carbide. It has been suggested that these be used as quantum sensors of the magnetic field and temperature with a sub-nanometer spatial resolution, as optically pumped masers, as optical and spin labels, as qubits in quantum computing, and as single-photon sources. Numerous capabilities of such spin centers are still to be discovered.

### Acknowledgements

We express our appreciation to our collaborators for their contribution to the papers cited here. This study was supported by the Russian Science Foundation (grant No. 14-12-00859) and the Russian Academy of Sciences.

### References

1. Zavoisky E J. *Phys. USSR* **9** 211 (1945)
2. Gruber A et al. *Science* **276** 2012 (1997)
3. Jelezko F et al. *Appl. Phys. Lett.* **81** 2160 (2002)
4. Jelezko F et al. *Phys. Rev. Lett.* **92** 076401 (2004)
5. Jelezko F, Wrachtrup J *Phys. Status Solidi A* **203** 3207 (2006)
6. Awschalom D D, Flatté M E *Nature Phys.* **3** 153 (2007)
7. Hanson R, Awschalom D D *Nature* **453** 1043 (2008)
8. Koenraad P M, Flatté M E *Nature Mater.* **10** 91 (2011)
9. Veinger A I et al. *Sov. Phys. Semicond.* **13** 1385 (1979); *Fiz. Tekh. Poluprovodn.* **13** 2366 (1979)
10. Vainer V S, Il'in V A *Sov. Phys. Solid State* **23** 2126 (1981); *Fiz. Tverd. Tela* **23** 3659 (1981)
11. von Bardeleben H J et al. *Phys. Rev. B* **62** 10126 (2000)
12. von Bardeleben H J et al. *Phys. Rev. B* **62** 10841 (2000)
13. Wagner M t et al. *Phys. Rev. B* **62** 16555 (2000)
14. Mizuochoi N et al. *Phys. Rev. B* **66** 235202 (2002)
15. Orlinski S B, Schmidt J, Mokhov E N, Baranov P G *Phys. Rev. B* **67** 125207 (2003)
16. Baranov P G et al. *JETP Lett.* **82** 441 (2005); *Pis'ma Zh. Eksp. Teor. Fiz.* **82** 494 (2005)
17. Carlos W E et al. *Phys. Rev. B* **74** 235201 (2006)
18. Baranov P G et al. *JETP Lett.* **86** 202 (2007); *Pis'ma Zh. Eksp. Teor. Fiz.* **86** 231 (2007)
19. Baranov P G et al. *Phys. Rev. B* **83** 125203 (2011)
20. Weber J R et al. *Proc. Natl. Acad. Sci. USA* **107** 8513 (2010)
21. DiVincenzo D *Nature Mater.* **9** 468 (2010)
22. Koehl W F et al. *Nature* **479** 84 (2011)
23. Soltamov V A et al. *Phys. Rev. Lett.* **108** 226402 (2012)
24. Riedel D et al. *Phys. Rev. Lett.* **109** 226402 (2012)
25. Baranov P G et al. *Mater. Sci. Forum* **740–742** 425 (2013)
26. Fuchs F et al. *Sci. Rep.* **3** 1637 (2013)
27. Kraus H et al. *Nature Phys.* **10** 157 (2014)
28. Kraus H et al. *Sci. Rep.* **4** 5303 (2014)
29. Falk A L et al. *Nature Commun.* **4** 1819 (2013)
30. Hain T C et al. *J. Appl. Phys.* **115** 133508 (2014)
31. Soltamov V A et al. *Phys. Rev. Lett.* **115** 247602 (2015)